Airborne Imaging Spectrometer HySpex

Deutsches Zentrum für Luft- und Raumfahrt e.V. (DLR)
Remote Sensing Technology Institute (IMF) [*]

Instrument Scientist:
- Claas H. Köhler, IMF, DLR Oberpfaffenhofen, Germany
  phone: +49 8153 28 1274, email: claas.koehler@dlr.de

Abstract: The Remote Sensing Technology Institute (IMF) of the German Aerospace Center (DLR) operates an airborne imaging spectrometer system called HySpex. Owing to its accurate calibration, the system is well suited for benchmark reference measurements and feasibility studies for Earth observation applications. The sensor also serves as simulator for the upcoming German satellite mission EnMAP. HySpex covers the spectral range from the visible and near infrared (VNIR) to the short wave infrared (SWIR) and it has been extensively characterised with numerous measurements in the IMF calibration laboratory (CHB). The HySpex instrument is made available to interested third party users through the user service Optical Airborne Remote Sensing and Calibration Homebase (OpAiRS).

1 Introduction

In 2011 the IMF procured an airborne imaging spectrometer system with the intention to investigate potential earth observation applications for the German satellite mission EnMAP[1]. This HySpex system purchased from the Norwegian Company Norsk Elektro Optikk A/S (NEO) features two different cameras covering the VNIR and SWIR spectral domain. Both cameras have been extensively characterised at IMF in cooperation with the National German Metrology Institute (PTB). The result is a very well characterised high precision instrument suited for benchmark earth observation applications. Owing to its high spatial and spectral resolution, the system is used mainly for feasibility studies of novel remote sensing applications over land and water, and for the validation of satellite measurements. HySpex is also available to external customers and research facilities (see chapter 4).

---

[1]www.enmap.org

2 System Overview

The following sections describe the individual components of the HySpex sensor system. Section 2.1 introduces the spectrometer systems and summarizes the results of extensive characterisation and calibration measurements performed in the Calibration Homebase (CHB, cf. DLR Remote Sensing Technology Institute., 2016). Since an in depth treatment of the afore mentioned efforts can be found in Lenhard, Baumgartner, & Schwarzmaier (2015) and Lenhard, Baumgartner, Gege, et al. (2015), the interested reader is referred to these publications for details. Section 2.2 is dedicated to the description of the navigation system used for absolute georeferencing of the acquired image data. Finally, we conclude with a brief overview of the experimental instrumental setup in section 2.3.
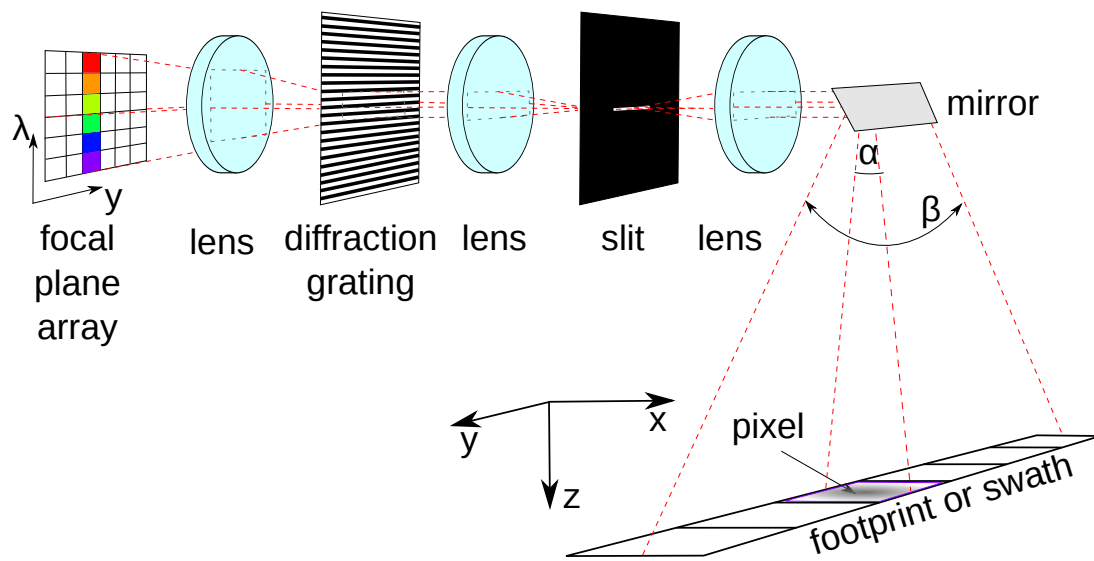
2.1 Spectrometer System

Figure 1: Working principle of a pushbroom sensor: The spectrum of the Gray shaded pixel is mapped to the coloured column on the focal plane array. Movement along the flight direction x allows formation of an image through combination of consecutive footprints. The field of view β determines the swath width while the instantaneous field of view α is related to the size of individual pixels.

The spectrometer system consists of two individual sensors: a HySpex VNIR-1600 covering the VNIR spectral domain and a SWIR-320m-e for the SWIR. Both imaging spectrometers are pushbroom sensors as shown in fig. 1: the footprint of the sensor approximately forms a straight line subdivided into a number of spatial pixels. The radiation stemming from each pixel is decomposed into its spectral components by means of a grating such that the one-dimensional field of view (FOV, labelled β in fig. 1) is mapped to a two dimensional (λ, y) intensity distribution in the focal plane. This intensity distribution can be measured using any two dimensional focal plane array (FPA) such as a charge coupled device (CCD) used in typical camera systems. Each image acquired by the FPA is called a frame.

The second spatial dimension (x or along track) required to form an image is obtained by subsequent acquisition of consecutive lines in combination with a movement perpendicular to the line of pixels spanned by the FOV. Following this definition the spatial dimension y is consequently referred to as across track.To characterise the size of an individual pixel, the angle α is typically introduced as instantaneous field of view (IFOV) in close analogy to the FOV. Note that two IFOVs (along track & across track) are required to characterise each pixel although fig. 1 lacks display of the latter for the sake of clarity.

2.1.1   HySpex VNIR-1600

The HySpex VNIR-1600 features a silicon CCD detector covering the spectral range $416 - 992$ nm with 160 channels. This results in a spectral sampling interval of 3.6 nm. The spectral resolution ranges from 3.5 nm at nadir to approximately 6 nm at the outer edge of the swath. The detector is equipped with two 12 bit digital converters, each processing one half of the CCD. The VNIR camera features three spectral (hardware) binning modes: $2\times$, $4\times$ and $8\times$. Here $n\times$ binning implies that n spectral detector elements are averaged to obtain a single channel. $n\times$ binning reduces spectral resolution by a factor of n in exchange for a higher maximum frame rate, an improved signal-to-noise ratio (SNR) and a reduced data volume. The maximum frame rate of the VNIR-1600 ranges from 135 Hz using $2\times$ binning to 160 Hz at $4\times$ or $8\times$ binning.

The HySpex VNIR sensor maps its total FOV of 16.7° onto 1600 spatial pixels. The FOV can be increased to 34.5° with a removable FOV expander lens. Table 1 provides an overview of key geometric characteristics of the VNIR camera at two typical flight altitudes. It should be noted that the VNIR-1600 pixels are not square but rectangular in shape owing to the along track IFOV being approximately twice as large as the across track IFOV.

		Altitude above Ground				
		1000 m			2000 m	
	Spatial Resolution		Swath	Spatial Resolution		Swath
	Along [m]	Across [m]	Width [m]	Along [m]	Across [m]	Width [m]
Mean	0.29 (0.64)	0.17 (0.37)	294 (620)	0.57 (1.28)	0.33 (0.74)	589 (1240)
Std. Dev.	0.03 (0.18)	0.02 (0.05)	0.04 (0.17)	0.06 (0.35)	0.03 (0.1)	0.09 (0.34)
Min	0.25 (0.44)	0.13 (0.27)	294 (620)	0.49 (0.88)	0.25 (0.54)	589 (1239)
Max	0.41 (1.22)	0.2 (0.64)	294 (620)	0.82 (2.44)	0.41 (1.28)	589 (1240)

Table 1: Selection of geometric parameters for the HySpex VNIR 1600 at two typical flight altitudes. Values in brackets are obtained with FOV expander lens attached.

In order to correct detector non-linearity and stray light, several measurements were performed in cooperation with PTB within the framework of the EURAMET project. Lenhard, Baumgartner, Gege, et al. (2015) elaborate on the associated methods and discuss the achievable improvements for the exemplary application of inland water depth retrieval.

2.1.2   HySpex SWIR-320m-e

The HySpex SWIR-320m-e is equipped with a mercury cadmium telluride (MCT) detector with 256 channels distributed over the spectral range $968 - 2498$ nm at a sampling interval of 6 nm and a spectral resolution of $5.6 - 7.0$ nm. The detector has a single integrated digital converter with a dynamic range of 14 bit. In contrast to the VNIR-1600, the SWIR-320m-e features pixels approximately square in shape. At 13.2° its total FOV is slightly smaller than the VNIR-1600 FOV, hence leading to a reduced swath width at identical altitudes compared to the VNIR camera. In the overlap region of the two swaths each of the 320 HySpex SWIR pixels covers approximately 4 VNIR pixels across-track and two VNIR pixels along track. As is the case for the VNIR spectrometer, the SWIR sensor can be equipped with a removable FOV expander lens. The expander increases the FOV to 27.2°, thus approximately doubling the size of each pixel. The SWIR-320m-e acquires images up to a maximum frame rate of 99 Hz. Table 2 summarises several geometric properties of the HySpex SWIR-320m-e in complete analogy to table 1 for the VNIR.

	Altitude above Ground					
	1000 m			2000 m		
	Spatial Resolution		Swath	Spatial Resolution		Swath
	Along [m]	Across [m]	Width [m]	Along [m]	Across [m]	Width [m]
Mean	0.54 (1.11)	0.70 (1.44)	231 (484)	1.09 (2.21)	1.39 (2.88)	462 (967)
Std. Dev.	0.02 (0.04)	0.04 (0.10)	0.05 (0.07)	0.04 (0.08)	0.08 (0.20)	0.11 (0.14)
Min	0.52 (1.04)	0.63 (1.31)	231 (483)	1.03 (2.07)	1.25 (2.62)	462 (967)
Max	0.61 (1.36)	0.82 (1.79)	231 (483)	1.23 (2.73)	1.64 (3.59)	462 (967)

Table 2: Selection of geometric parameters for the HySpex SWIR-320m-e at two typical flight altitudes. Values in brackets are obtained with FOV expander lens attached.

2.2 Position and Attitude Determination

In order to provide accurate georeferencing for the acquired data, the HySpex system is equipped with a high precision iTraceRT-F200 coupled INS/GPS navigation system manufactured by the German company iMAR. The iTrace features a high precision Novatel SPAN GPS receiver with an integrated fiber optical gyro based inertial measurement unit (IMU). The GPS accuracy can be increased with a built-in Omnistar receiver for real time kinematic processing. The iMAR IMU is rigidly attached to the sensor assembly on a PAV30 stabilizing platform. The latter reduces the influence of aircraft motion and wind correction angle on the image data. An integrated Kalman Filter processes the INS and GPS/Omnistar measurements online yielding position and attitude at a rate of 200 Hz in real time. A calibration flight over an area with well known reference points is performed after each installation into an aircraft to determine the exterior orientation (i.e. sensor orientation with respect to the navigation system). This process is also known as boresight calibration. The synchronisation of HySpex and navigation data is realised through TTL pulses sent from the HySpex data acquisition unit to the iTrace IMU. The logged navigation data is interpolated based on the afore mentioned time marks in a post-processing step to obtain camera position and attitude at the time of acquisition for each frame.
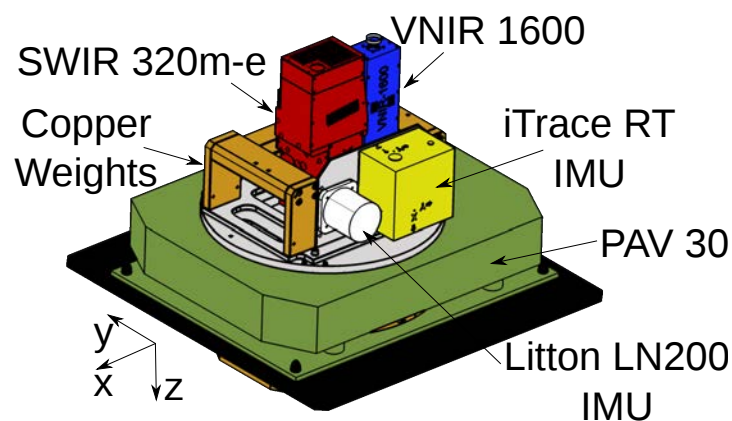
2.3 Experimental Setup

Figure 2: Experimental setup of the HySpex sensor system. *x* is the flight direction and *z* is nadir.

The experimental setup of the HySpex sensor system is shown in figure 2. Both sensors are mounted facing nadir on the Leica PAV30 gyro stabilized camera mount. The iMAR IMU used for georeferencing and the Litton LN-200 IMU aiding PAV30 operation are both rigidly attached to the sensor assembly. The HySpex Data acquisition unit is installed in a DLR F20 rack (not shown) along with an Applanix POSAV4

integrated navigation system. The POSAV4 actuates the PAV30 based on the Litton IMU measurements. Specifically designed weights have been added to the sensor system to move gross weight, center of gravity and all inertial moments into the operational envelope of the PAV30. Aircraft guidance during survey flights is provided by an IGI CCNS4 system.

The experimental setup described above is certified on two DLR research aircraft: A Cessna 208 Grand Caravan (D-FDLR) and a Dornier 228-212 (D-CFFU). The supplemental type certificate for the D-CFFU allows the optional inclusion of the 3K camera system described by Kurz et al. (2012), thus allowing simultaneous acquisition of high resolution RGB images in addition to the HySpex spectra. The 3K camera data can e.g. be used to infer a digital elevation model from multi-angle observations. Two to three operators are required during survey flights to operate the experimental equipment.

3   Data Processing

Data processing is organised in several steps commonly referred to as levels:
- **Level 0**: Raw data recorded by the HySpex sensor system
- **Level 1A**: Raw spectra with synchronised navigation data for each Hyspex frame
- **Level 1B**: At-sensor radiance including navigation data for georeferencing
- **Level 1C**: Orthorectified at-sensor radiance
- **Level 2A**: Orthorectified surface reflectance

The content of the products listed above and their respective data formats are described in detail in the HySpex Product Guide (Köhler & Schneider, 2015).

Apart from the Level 0 to Level 1A pre-processing– which essentially consists in synchronisation of navigation data and HySpex images– the entire processing chain has been implemented in the CATENA environment (Krauß, 2014; Krauß et al., 2013) developed at IMF . CATENA allows for non-supervised fully automated image processing based on the accumulated IMF expertise in operational data processing for various optical sensors.

In a first step, the Level 1A to Level 1B processor converts the raw digital numbers recorded by the sensor to the calibrated at-sensor radiance. This encompasses a system correction for several sensor artefacts such as viewing geometry for each pixel, spectral response for each channel, detector nonlinearity and stray light based on the sensor characterisation described in chapter 2.1. To achieve a very high co-registration accuracy, the individual images recorded by the VNIR-1600 and SWIR-320m-e sensors are matched onto each other using the BRISK algorithm of Leutenegger et al. (2011) before orthorectification with the DLR Ortho software (Müller et al., 2005). Details of this Level 1C processing step can also be found in Schwind et al. (2014). To mitigate the radiative effect of gases, aerosols and clouds on the image data, the Level 1C data is atmospherically corrected with ATCOR4 (Richter et al., 2011) for the Level 2A product. In addition to the processing steps described above, the Level 0 product is archived in the German Satellite Data Archive (see Kiemle et al., 2014) to ensure permanent availability of the data for future reanalysis.

4   HySpex Access through the User Service OpAiRS

The IMF offers the HySpex sensor system to third party customers through its ISO 9001 certified user service Optical Airborne Remote Sensing and Calibration Homebase (OpAiRS). In close cooperation with the DLR flight facilities, OpAiRS offers end-to-end capabilities from survey planning via campaign management and sensor operation to data processing. Additionally, we aim to ensure high data quality through regular measurements of our sensors in the CHB. OpAiRS allows users to access the IMF expertise accumulated in over 20 years of optical airborne remote sensing during operation of the sensors DAIS 7915, ROSIS, HyMap and lately HySpex.

Potential users from abroad might be interested in the trans national access program of the European Facility for Airborne Research (EuFAR[2]), which features the DLR HySpex as one of its instruments.

---

[2]www.eufar.net

Scientists interested in cooperative surveys with the HySpex sensors (possibly in combination with the 3K camera system) are invited to contact us via opairs@dlr.de. Further information is also available on the OpAiRS website http://www.dlr.de/opairs.

References

DLR Remote Sensing Technology Institute. (2016). The Calibration Home Base for Imaging Spectrometers. *J. Lrg.-Scale Res. Fac.*, *2*(A82). http://dx.doi.org/10.17815/jlsrf-2-137

Kiemle, S., Molch, K., Schropp, S., Weiland, N., & Mikusch, E. (2014). Big data management in Earth Observation: the German Satellite Data Archive at DLR. In P. Soille & P. Marchetti (Eds.), *Big data from space, bids'14* (pp. 46–49). Publications Office of the European Union. http://dx.doi.org/10.2788/1823

Köhler, C. H., & Schneider, M. (2015, 22 May). *HySpex Product Guide* (Issue No. 1.1). Deutsches Zentrum für Luft- und Raumfahrt. Retrieved from http://www.dlr.de/opairs

Krauß, T. (2014, April). Six Years Operational Processing of Satellite data using CATENA at DLR: Experiences and Recommendations. *Kartographische Nachrichten*, *64*(2), 74–80. Retrieved from http://elib.dlr.de/88864/

Krauß, T., d'Angelo, P., Schneider, M., & Gstaiger, V. (2013, May). The Fully Automatic Optical Processing System CATENA at DLR. In C. Heipke, K. Jacobsen, F. Rottensteiner, & U. Sörgel (Eds.), *ISPRS Hannover workshop 2013* (Vol. XL-1/W, pp. 177–181). Copernicus Publications. http://dx.doi.org/10.5194/isprsarchives-XL-1-W1-177-2013

Kurz, F., Türmer, S., Meynberg, O., Rosenbaum, D., Runge, H., Reinartz, P., & Leitloff, J. (2012, April). Low-cost optical Camera System for real-time Mapping Applications. *Photogrammetrie Fernerkundung Geoinformation*, *Jahrgang 2012*(2), 159–176. http://dx.doi.org/10.1127/1432-8364/2012/0109

Lenhard, K., Baumgartner, A., Gege, P., Nevas, S., Nowy, S., & Sperling, A. (2015, November). Impact of Improved Calibration of a NEO HySpex VNIR-1600 Sensor on Remote Sensing of Water Depth. *IEEE Trans. Geosci. Remote Sens.*, *53*(11), 6085-6098. http://dx.doi.org/10.1109/TGRS.2015.2431743

Lenhard, K., Baumgartner, A., & Schwarzmaier, T. (2015, April). Independent Laboratory Characterization of NEO HySpex Imaging Spectrometers VNIR-1600 and SWIR-320m-e. *IEEE Trans. Geosci. Remote Sens.*, *53*(4), 1828-1841. http://dx.doi.org/10.1109/TGRS.2014.2349737

Leutenegger, S., Chli, M., & Siegwart, R. Y. (2011, November). BRISK: Binary Robust invariant scalable keypoints. In *2011 international conference on computer vision* (p. 2548-2555). http://dx.doi.org/10.1109/ICCV.2011.6126542

Müller, R., Lehner, M., Reinartz, P., & Schroeder, M. (2005, May). Evaluation of Spaceborne and Airborne Line Scanner Images using a Generic Ortho Image Processor. In C. Heipke, K. Jacobsen, & M. Gerke (Eds.), *High Resolution Earth Imaging for Geospatial Information, Hannover* (Vol. Vol. XXXVI). Retrieved from http://elib.dlr.de/18927/

Richter, R., Schläpfer, D., & Müller, A. (2011, July). Operational Atmospheric Correction for Imaging Spectrometers Accounting for the Smile Effect. *IEEE Trans. Geosci. Remote Sens.*, *49*(5), 1772–1780. http://dx.doi.org/10.1109/TGRS.2010.2089799

Schwind, P., Schneider, M., & Müller, R. (2014, November). Improving HySpex Sensor Co-Registration Accuracy using BRISK and Sensor-model based RANSAC. In C. Toth, T. Holm, & B. Jutzi (Eds.), *Pecora 19 Symposium in conjunction with the Joint Symposium of ISPRS Technical Commission I and IAG Commission 4* (Vol. XL-1, pp. 371–376). ISPRS Archive. http://dx.doi.org/10.5194/isprsarchives-XL-1-371-2014